NACA RM L56L11

NACA

RESEARCH MEMORANDUM

TWO-DIMENSIONAL TRANSONIC INVESTIGATION OF FLOWS AND FORCES ON A 9-PERCENT-THICK AIRFOIL WITH 30-PERCENT-CHORD FLAP

By Walter F. Lindsey and Robert G. Pitts

Langley Aeronautical Laboratory
Langley Field, Va.

NATIONAL ADVISORY COMMITTEE
FOR AERONAUTICS

WASHINGTON

February 19, 1957
Declassified February 10, 1959

1J

NACA RM L56L11

NATIONAL ADVISORY COMMITTEE FOR AERONAUTICS

RESEARCH MEMORANDUM

TWO-DIMENSIONAL TRANSONIC INVESTIGATION OF FLOWS AND FORCES ON A 9-PERCENT-THICK AIRFOIL WITH 30-PERCENT-CHORD FLAP

By Walter F. Lindsey and Robert G. Pitts

SUMMARY

An investigation has been conducted to measure the pressures on and to observe by schlieren photography the flow about an NACA 65A009 airfoil with a 30-percent-chord trailing-edge flap in transonic flow. The investigation was made in a two-dimensional slotted tunnel at Mach numbers from 0.7 to about 1.2. The corresponding Reynolds number range was from 2.4×10^6 to 2.8×10^6. Data were obtained at angles of attack to 10° and flap deflections to 30°.

The results indicate that the flows over the flap are subject to changes from subsonic to supersonic values, which are dependent on combinations and variations in Mach number, angle of attack, and flap deflection. The resulting effect on the forces is to produce erratic variations that are not subject to any simple correlation factors. The highest flap normal-force coefficients observed in this investigation were around 1.5 and occurred in the highest flap-deflection and Mach number ranges of the tests.

INTRODUCTION

The determination of aerodynamic loads on flaps and controls is a basic problem that confronts aircraft designers. These loads, in pure subsonic and pure supersonic flow, can be readily estimated by accepted theories and existing experimental data. For transonic speeds, however, there are no theoretical solutions and very little experimental data, especially at Mach numbers around 1.0 or for large flap deflections. Variations in angle of attack, flap deflection, and Mach number in this speed range combine in a large number of ways to produce many different

flow patterns. The multiplicity of flow patterns do not lend themselves to analytical solutions by adaptations of either the subsonic theory or the supersonic theory.

In order to provide some information at transonic speeds on loads, load variations, and maximum loadings, a limited investigation has been conducted on an NACA 65A009 airfoil with a 30-percent-chord plain unsealed trailing-edge flap in two-dimensional flow. The investigation was conducted at Mach numbers between 0.7 and 1.2 at positive angles of attack of 0°, 5°, and 10° and at downward flap deflections of 0°, 5°, 10°, 20°, and 30°. The Reynolds numbers of the tests were from 2.4×10^6 to 2.8×10^6.

SYMBOLS

c_h	flap hinge-moment coefficient, based on flap chord
$c_{m_{c/4}}$	section pitching-moment coefficient about quarter-chord axis
c_n	section normal-force coefficient
c_{n_f}	flap normal-force coefficient, based on flap chord
M	free-stream Mach number
α	angle of attack, deg
δ	angle of flap deflection relative to airfoil chord, deg
C_p	pressure coefficient, $\frac{\text{Local static pressure - Free-stream static pressure}}{\text{Free-stream dynamic pressure}}$
$C_{p_{cr}}$	pressure coefficient for local Mach number equal to 1.0

APPARATUS, MODEL, AND TESTS

Tests were conducted in the Langley airfoil test apparatus shown in figure 1. The facility has a test section 4 inches wide and 19 inches high with upper and lower walls slotted. Total width of slots at the test section is one-eighth of the 4-inch width of the test section. The

apparatus operates on the direct blow-down principle and uses compressed air that has been dried and stored at 300 pounds per square inch.

The tests were made at a stagnation pressure of 26 pounds per square inch absolute. In the calibrations of the apparatus, static pressures were measured through the empty test region. At a Mach number of 1.25 and a stagnation pressure of 26 pounds per square inch absolute, the Mach numbers were constant (variations less than ±0.002) for a distance of one chord length ahead of and behind the model midchord. (The model spanned the 4-inch test section width.)

The model investigated was an NACA 65A009 airfoil section (ordinates in ref. 1) with a 30-percent-chord trailing-edge flap (fig. 2). The model had both a span and a chord of 4 inches and had static-pressure orifices at 1.25-, 2.50-, 5.00-, 7.50-, 10-, 15-, 20-, 25-, 30-, 35-, 40-, 45-, 50-, 55-, 60-, 65-, 70-, 75-, 80-, 85-, 90-, and 95-percent-chord stations on both upper and lower surfaces.

The flap was attached to the solid brass model by means of a hinge similar to a piano hinge located on the chord of the symmetrical airfoil. The hinge pin extended through the tunnel wall and was rotated to deflect the flap. A check was made after each test, and the method of setting and holding flap deflections seemed satisfactory. Because of the length and the small size (0.238-inch diameter) of the pin there existed some possibility at high flap deflections of slight angle deviations due to torsional deflection of the hinge pin for which no correction has been applied.

Pressure-distribution data were obtained on a mercury manometer and photographically recorded. Coefficients for section normal force, pitching moment, flap hinge moment, and flap normal force were obtained by integration from the pressure-distribution measurements. The pressure distributions on the forebody and on the flap were integrated separately to provide two normal-force-coefficient components and two moment coefficients. The normal-force coefficient obtained for the flap was the flap normal-force coefficient c_{n_f}. The section normal-force coefficient was computed by adding the forebody normal-force coefficient to $0.3c_{n_f} \cos \delta$.

The tunnel-wall boundary layer flowed over the model at the model wall junctures. Preliminary tests in a similar test facility and comparisons of data with that from other sources (see ref. 1) indicate that the end effects are small. The data were obtained at Mach numbers from 0.7 to 1.2 for angles of attack of 0°, 5°, and 10° for flap deflections of 0°, 5°, 10°, 20°, and 30°. The Reynolds number of the flow, based on the 4-inch model chord, ranged from 2.4×10^6 to 2.8×10^6.

Schlieren motion pictures of the flow past the model (without pressure orifices) were made for a few combinations of angles of attack and flap deflections. These photographs and other similar investigations (refs. 1 and 2) indicated that the boundary layer on the model ahead of the shock was laminar.

RESULTS

Pressure distributions along the chord of the model for representative Mach numbers, angles of attack, and flap deflections are shown in figures 3 and 4. Schlieren photographs are shown in figures 3 and 5. Variations with Mach number of section normal force, section pitching moment, flap normal force, and flap hinge moment for different angles of attack and flap deflections are presented in figure 6. Figures 7 and 8 show the variation of section normal force and flap normal force with angle of attack and flap deflection for Mach numbers throughout the test range. Figure 9 shows highest values of flap normal force obtained over the Mach number range of the investigation. Figure 9 also presents the maximum and the minimum measured pressure coefficients on the flap for various Mach numbers as compared with computed pressure coefficients at stagnation behind a normal shock for the stream Mach number concerned and at vacuum.

DISCUSSION

These two-dimensional data obtained in a one-eighth open slotted two-dimensional test section (fig. 1) are subject to corrections. The largest correction applies to the angles of attack. A comparison of data from different test facilities indicated that no reliable corrections are available at present. The data are therefore presented in uncorrected form.

The flow patterns over a model can be defined as purely subsonic, purely supersonic, or transonic. The range of this investigation included both purely subsonic and transonic flows. The transonic or mixed-flow range is of greatest interest because of the unpredictable character of the flow. The distribution of pressures over the model shown in figures 3 and 4 in the speed range of primary interest is representative of the deviations from and conformance to well-known conditions.

Effect of Flaps on Flows

Upper surface.- The flow along the upper surface of the model (figs. 3, 4, and 5) follows the characteristic pattern of transonic flows

past thick and moderately thick airfoils (refs. 1 and 3). The expansion angle at the hinge axis formed by the downward deflection of the flap assists in producing flow separation over the rear part of the model and greatly reduces the rate (with free-stream Mach number) of rearward movement of the position of the rapid compression associated with the shock at the rear of the supersonic flow region. At a given angle of attack, increasing the Mach number produces increased angle of separation (angle between the flow boundary and the model surface) without affecting the location of the rapid surface pressure rise even though the shock moves rearward along the separation boundary. (See $M = 0.89$ and $M = 0.94$, fig. 3.)

With further increase in Mach number and its attendant decrease in pressure behind the model, the flow first starts expanding around the corner at the hinge axis and reduces the angle of separation. Later the chordwise extent of separation starts decreasing. This process continues with increasing Mach number until the flow is completely closed in around the hinge axis and supersonic flow exists along the flap upper surface. The expansion around the hinge axis is approximately 95 percent of the turning angle predicted by supersonic-flow theory for a Prandtl-Meyer turn. An analysis of all the data obtained showed that the Mach number at which the upper-surface shock reaches the trailing edge increases with both increasing flap deflection and increasing angle of attack. See for example photographs at $M = 1.04$ and $\delta = 7.75^\circ$ for $\alpha = 0^\circ$ (fig. 3) and $\alpha = 10^\circ$ (fig. 5).

At Mach numbers of 0.84 and 0.97 and an angle of attack of 0° (fig. 4), an increase in flap deflection above 5° produces a decrease in the pressures on the flap even though the flow remains separated from the flap. This may be attributed to the pumping action of the increased vorticity of the wake of the separated flow. As a result, the upper surface of the flap contributes to an increase in flap normal force with increasing flap deflection regardless of the existence of flow separation.

Lower surface.- The flow along the lower surface differs from that on the upper surface because positive flap deflections form a local concavity or corner at the hinge axis. A purely subsonic flow may flow into and out of the corner, but a supersonic flow cannot become established on the flap until the local surface Mach number is sufficiently high to permit flow attachment within the corner. The limiting conditions of the flow angle into the corner and the required local Mach number can be estimated from oblique shock theory. Analysis of pressure measurements for conditions of attached shock at the hinge axis (representative examples are presented in fig. 4) showed that the flow-angle changes based on the pressures ahead of and behind the hinge axis and on oblique-shock theory were around 70 percent of the flap deflections or theoretical values. The difference in percent attainment of theoretical values between upper-surface expansions and lower-surface

compressions can be attributed to pressure-gradient effects on the boundary-layer conditions.

An increase in flap deflection requires an increase in the local Mach number for the supersonic flow to flow into and out of the corner. An increase in angle of attack produces a reduction in the local Mach numbers along the lower surface. Thus, increases in either angle of attack or flap deflection delay the development of supersonic flows on the flap to higher free-stream Mach numbers. The increase in pressure from the 90- to 95-percent-chord stations, observed in some of the distributions, appears to result from an erratic variation in the pressure at the 90-percent-chord station which cannot be explained.

General.- For incompressible flows $c_{n_f} = f_1(\alpha) + f_2(\delta)$ (where $f(\alpha)$ is a function of α, ref. 3) and the flap-load distribution is triangular with its center of pressure at the one-third flap chord. This type of distribution persists to Mach numbers well in excess of the critical value (fig. 4, $\alpha = 0^\circ$, $\delta = 5^\circ$, $M = 0.84$). At supersonic speeds $c_{n_f} = (\alpha + \delta)\left[f_3(M) - f_4(M)\tau\right]$ (where τ is a trailing-edge shape factor based on Busemann's second-order theory, ref. 5). The load distribution is rectangular with its center of pressure at the 50-percent-flap-chord station. The rectangular load distribution is shown in figure 4 to occur at free-stream Mach numbers greater than 1.0 although the separate flap surfaces exhibit the supersonic type of distribution at Mach numbers less than 1.0 (fig. 4(a)). The changes from triangular to rectangular loadings occur over a range of speeds within the transonic Mach number range. The resulting loadings which may be called transitional loadings, vary in shape, but are predominantly trapezoidal.

A comparison of the flap loads on the basis of equal values of $(\alpha + \delta)$ is still of interest and can be made from figure 4. For $(\alpha + \delta) = 10^\circ$ at the two low angles of attack of 0° and 5°, the flap-load distributions are similar at Mach numbers greater than 1.0. The differences that exist at a given Mach number are a slightly more forward position of the abrupt compression on the upper surface at $\alpha = 5^\circ$ and the result on the lower-surface flow of the decelerating effect of an increase in the angle of attack. The latter effect is evident in a delay in the establishment of supersonic flow into the corner. At an α of 10° and δ of 0° (fig. 4(b)) the flap loads, however, are very different. At the lower Mach numbers there is no similarity in the loads.

For $(\alpha + \delta) = 20^\circ$, the loads at $\alpha = 0^\circ$ and $\delta = 20^\circ$ are quite different from those at $\alpha = 10^\circ$ and $\delta = 10^\circ$. At a Mach number of 1.04 supersonic flow exists along the upper surface for the low-angle-of-attack condition, and separated flow is encountered on the flap at the high-angle-of-attack condition. (See fig. 5.) Because an increase in

α or δ or both increases the free-stream Mach number for attainment of the supersonic or rectangular flap-load distribution and broadens the Mach number range of transition from subsonic to supersonic loading, a simplified method of correlation of the changes in load is precluded.

These data also provide information on the extent of propagation of pressure influences around a model. It appears reasonable that the positive pressure field of the deflected flap could extend not only through the subsonic distributions along the lower surface of a model but also affect the flow around the leading edge and on the upper surface. Examination of the data for the upper surface pressure distribution in figures 4(a) and (b) at Mach numbers from 0.84 to 0.94 indicate that the effect of the flap flow field on the upper-surface forebody flow is very small and practically insignificant.

Additional general information on the flow is shown in figure 5 which shows the changes in flow through a Mach number range for the airfoil at an angle of attack of 10° and a flap deflection of 7.75°. The moving pictures showed that the flow along the upper surface was very unsteady at Mach numbers from 0.77 to 0.90. The unsteady flow is illustrated in figure 5 by the strip of moving pictures taken at a Mach number of 0.84 which shows the separation point oscillating from the leading edge to about the 25-percent-chord station and shows simultaneous variations in the shock strength. Similar conditions exist at Mach numbers of 0.87 and 0.89 although the separation point has moved rearward and the oscillations occur less frequently. These unsteady flows produce unsteady forces and contribute to buffeting. (See ref. 6.) The pressure-distribution diagrams (figs. 3 and 4) are time-average results and show only a general smoothing out of the pressure gradients as a result of the oscillating flow. As the Mach number is increased above 0.90, the separation point moves steadily rearward along with the shock to the hinge axis at $M = 1.04$. Further increases in Mach number produce a continuous decrease in the extent of separation.

Forces

Force and moment variations with Mach number.- The separation effects have a large influence on the aerodynamic characteristics of the airfoil. As the free-stream Mach number is increased, separation of the flow from the upper surface of the flap combined with the development of supersonic flow with its attendant reduction in static pressures on the lower surface of the flap caused the flap to be ineffective at $\alpha = 0^\circ$, $\delta = 5^\circ$, and Mach numbers from 0.94 to 0.97 (fig. 4(a)). The flap ineffectiveness is similar to the reversed loading observed on moderately thick airfoils (refs. 1 and 3) and is evident in the force coefficients in figure 6(a).

The ineffectiveness of the flap at $\delta = 5^\circ$ observed in the section normal-force-coefficient variation with Mach number is magnified by a flow change that is independent of separation effects. For an angle of attack of 0° and flap deflections of 5° and 10°, the rapid decrease in the section normal-force coefficient from Mach numbers around 0.85 to Mach numbers around 0.94 (fig. 6(a)) are a result of the development of supersonic flow and the rearward movement of the shock on the lower surface of the airfoil. (See also figs. 3 and 4(a).) The rise in section normal-force coefficient at Mach numbers from 0.97 to 1.0 is a result of gradual elimination of the separation and establishment of supersonic flow over the flap upper surface. The section normal-force coefficients ($\alpha = 0^\circ$, $\delta = 5^\circ$, and $\delta = 10^\circ$) at Mach numbers above 1.03 are entirely attributable to forces on the flap alone and are about 40 percent of the values at Mach numbers around 0.75.

At high flap deflections, 20° and 30°, the normal-force variation in figure 6(a) is considerably different from that at lower flap angles. There is a general decrease in section normal-force coefficient which can be attributed to a slow decrease in the flap effect on decelerating the flow on the lower surface, but the decrease in section normal-force coefficient is smaller because throughout the speed range at these high flap deflections the flow does not become supersonic over the entire forebody of the lower surface of the model. (See $\alpha = 0^\circ$ and $\delta = 20^\circ$, fig. 4(a).)

Increasing the angle of attack accentuates the high-flap-deflection form of force variation in that the changes are small and the deviations decrease. For $\alpha = 10^\circ$, the flow is essentially stalled along the upper surface at Mach numbers below 0.90 as indicated by figure 5; and, as a consequence, the force variations or the effect of flap deflections are less and the variations over the Mach number range are also less.

The variation of the flap normal-force coefficients with Mach number (fig. 6) differs from the section normal-force variation in that c_{n_f} tends to increase continually up to a Mach number around 1.0. This variation is a result of the change from the subsonic (triangular) to the transitional (trapezoidal) or the supersonic (rectangular) load distribution. For large flap deflections the same general result is obtained even though the change in load distribution is occurring only along the flap upper surface as shown in figure 4. At angles of attack greater than 0°, the flap normal-force coefficients follow the same general pattern as at the low angle and high flap deflections.

The flap hinge-moment coefficients form a similar pattern to the flap normal-force coefficients because the center-of-pressure travel is small. The total movement is from about the 30-percent-chord position at low Mach numbers to the 50-percent-chord position at the high Mach

numbers. The 30-percent-chord position corresponds closely to the basic triangular loading on the flap in incompressible flow. The 50-percent flap chordwise position corresponds to the rectangular load distribution for supersonic flow.

The data in figure 6 indicate that deflections of the flap (for $(\alpha + \delta) > 10^{\circ}$) reduce the erratic variations in section pitching-moment coefficient $c_{m_{c/4}}$ with Mach number and produce almost continuous increases in the negative moment coefficient with increasing Mach number up to sonic velocity. This behavior is similar to the effects of camber shown in reference 1 as would be expected. At Mach numbers greater than 1.0 the variations in $c_{m_{c/4}}$ are small because changes in the chordwise extent of supersonic flow region are small.

Normal-force variations with angle.- The section normal-force coefficients of the airfoil and their variations with angle of attack and flap deflection are shown in figures 7(a) and (b) for Mach numbers of 0.7, 0.8, 0.9, 1.0, 1.1, and 1.2. These results at free-stream Mach numbers less than 1.0 show, for constant but large flap deflections, maximum values of the section normal-force coefficient of about 1.4 that decreased with increases in Mach number. At $M = 1.0$, an increase is indicated in maximum c_n but the data are incomplete.

The trends in the variations of section normal-force coefficients with the flap deflection indicate for Mach numbers below 1.0 that section normal forces in excess of 1.4 are possible for flap deflections greater than 30° and at angles of attack around 5°. Flow separation from the airfoil leading edge was encountered at an angle of attack of 10°. At higher Mach numbers similar trends are indicated for increased flap deflections; however, the angle of attack should also increase.

Examination of the slopes of the curves in figures 7(a) and (b) shows that the variation with flap deflection is much more nonlinear than the variation with angle of attack. Of particular interest is the variation of the normal-force coefficient with flap deflection for a Mach number of 1.0 at zero angle of attack. From 0° to 10° flap deflections, the slope is moderate. In the range from 10° to 20° the slope is very large but decreases in the range from 20° to 30°. This variation in slope over the flap-deflection range is a result of variations in the flow patterns. Changes occur only in the flap load when the flap is deflected from 0° through 5° to almost 10°; no change occurs in the forebody load. Deflection of the flap from 10° to 20° induces the normal shock to move forward on the airfoil lower surface, causes a rapid increase in the pressure on the airfoil lower surface, and results in a consequent increase in section normal force. The maximum effect of this shock movement is attained at this Mach number for a flap deflection of 20°.

The pressure distributions (not shown) from 20° to 30° show the change in flow over the lower surface is extremely small; the effect on the upper-surface flow is slight, and consequently the change in section normal-force coefficient is small. Similar changes occur at lower flap deflections for angles of attack of 5° and to a much less extent at an angle of attack of 10°. These changes contribute to nonlinearities in the force variations with attitude through the transonic speed range.

In the variation of flap normal-force coefficient with flap deflection (fig. 8(b)) at a Mach number of 1.0, which corresponds to the condition discussed for the section normal-force coefficient, the flap normal-force coefficient follows the same pattern to a slight extent; direct correlation was not expected from the flow studies.

The variations of the flap normal-force coefficients with angle of attack at different flap deflections are quite irregular (fig. 8(a)) especially at Mach numbers of 1.0 and less. These large irregularities contribute to the nonlinear variations with flap deflection. Since the flap normal-force coefficients at angle-of-attack and flap-deflection combinations beyond the attainment of the maximum section normal-force coefficient are not important, the data of figure 8 have been examined for the conditions of an increase in the section normal-force coefficient. The trends in figure 8 indicate that increases in flap deflection at angles of attack around 5° would also be accompanied by increases in flap normal-force coefficient at Mach numbers less than 1.0. At Mach numbers greater than 1.0, however, an increase in both angle of attack and flap deflection which would be expected to increase the section normal-force coefficient may or may not produce increases in flap normal-force coefficient.

Maximum loads.- The data provide some information that can serve as a preliminary guide in the estimation of maximum flap loads. In figure 9 the variation with Mach number of the highest values of flap normal-force coefficients obtained within the limitations of this investigation are presented and show peak values of about 1.5. Throughout the range of Mach numbers it is observed that the combination of angle of attack and flap deflection required to produce the highest value changed over the speed range.

The maximum and minimum pressure coefficients (maximum negative and maximum positive) observed on the flap in this investigation provide information applicable to panel-load estimations. The variations with Mach number of these experimental limits are compared in figure 9 with the pressure coefficients for vacuum and with the pressure coefficients for the stagnation point on the airfoil. If these envelope curves for pressures are used to provide an estimate of flap normal force, large errors are introduced. At $M = 1.0$ the estimated value is 2.04, whereas

the experimental value of flap normal force is 1.48. The large difference occurs because the most positive pressure and the most negative pressure coefficients did not occur simultaneously. The most positive pressure coefficients on the lower surface are generally obtained under conditions of high angles and high flap deflections, whereas the more negative pressure coefficients are obtained at angles of attack where separation effects are not predominant.

CONCLUDING REMARKS

The results indicate that the local flows over the flap are subject to changes from subsonic to supersonic values which are dependent on combinations and variations in Mach number, angle of attack, and flap deflection. The resulting effect on the forces is to produce erratic variations that are not subject to any simple correlation factors.

The highest normal-force coefficients obtained in this investigation were around 1.4 for the airfoil and 1.5 for the flap. The highest flap normal-force coefficients occurred in the highest flap-deflection and Mach number ranges of the tests.

No correlation existed between maximum flap normal force and maximum and minimum pressures on the flap because the maximum and the minimum values occurred under different combinations of angle of attack and flap deflection.

Langley Aeronautical Laboratory,
National Advisory Committee for Aeronautics,
Langley Field, Va., November 28, 1956.

REFERENCES

1. Daley, Bernard N., and Dick, Richard S.: Effect of Thickness, Camber, and Thickness Distribution on Airfoil Characteristics at Mach Numbers up to 1.0. NACA TN 3607, 1956. (Supersedes NACA RM L52G31a.)

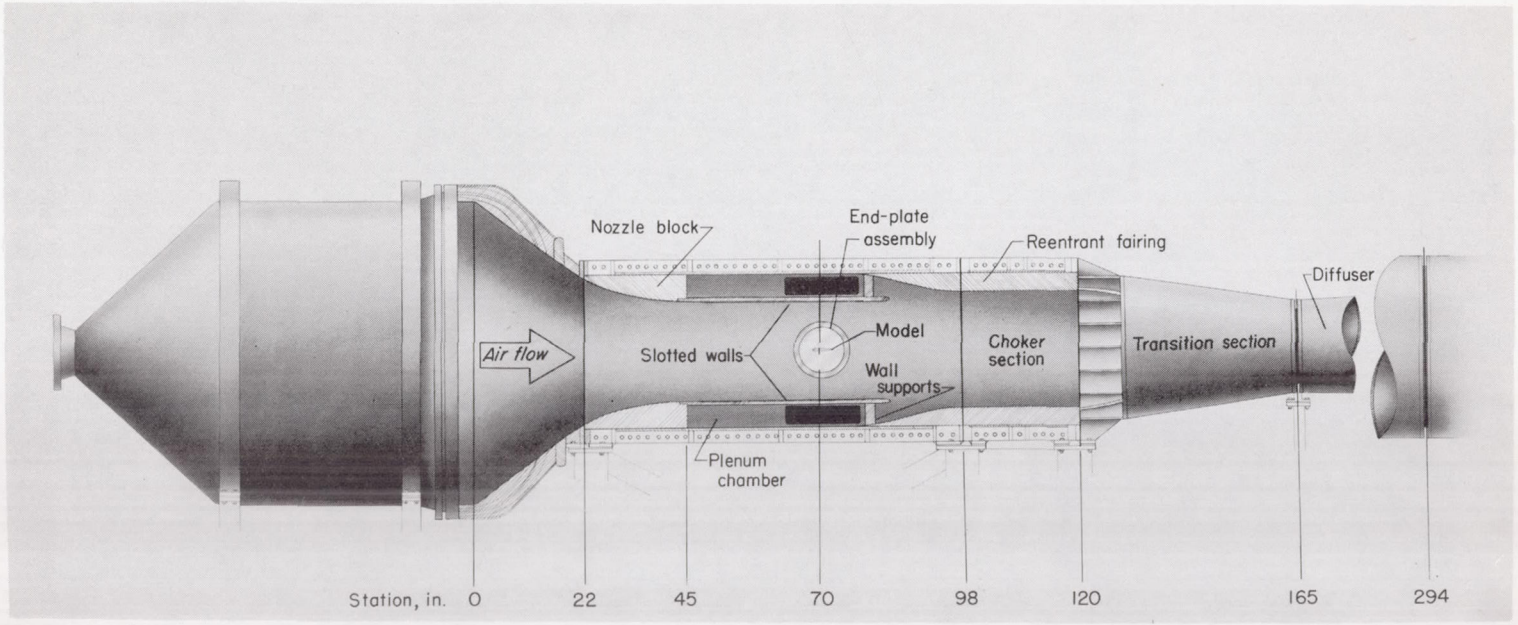
2. Lindsey, Walter F., and Johnston, Patrick J.: Some Observations On Maximum Pressure Rise Across Shocks Without Boundary-Layer Separation on Airfoils at Transonic Speeds. NACA TN 3820, 1956.

3. Lindsey, Walter F., and Dick, Richard S.: Two-Dimensional Chordwise Load Distributions at Transonic Speeds. NACA RM L51I07, 1952.

4. Glauert, H.: Theoretical Relationships for an Aerofoil With Hinged Flap. R. & M. No. 1095, British A.R.C., 1927.

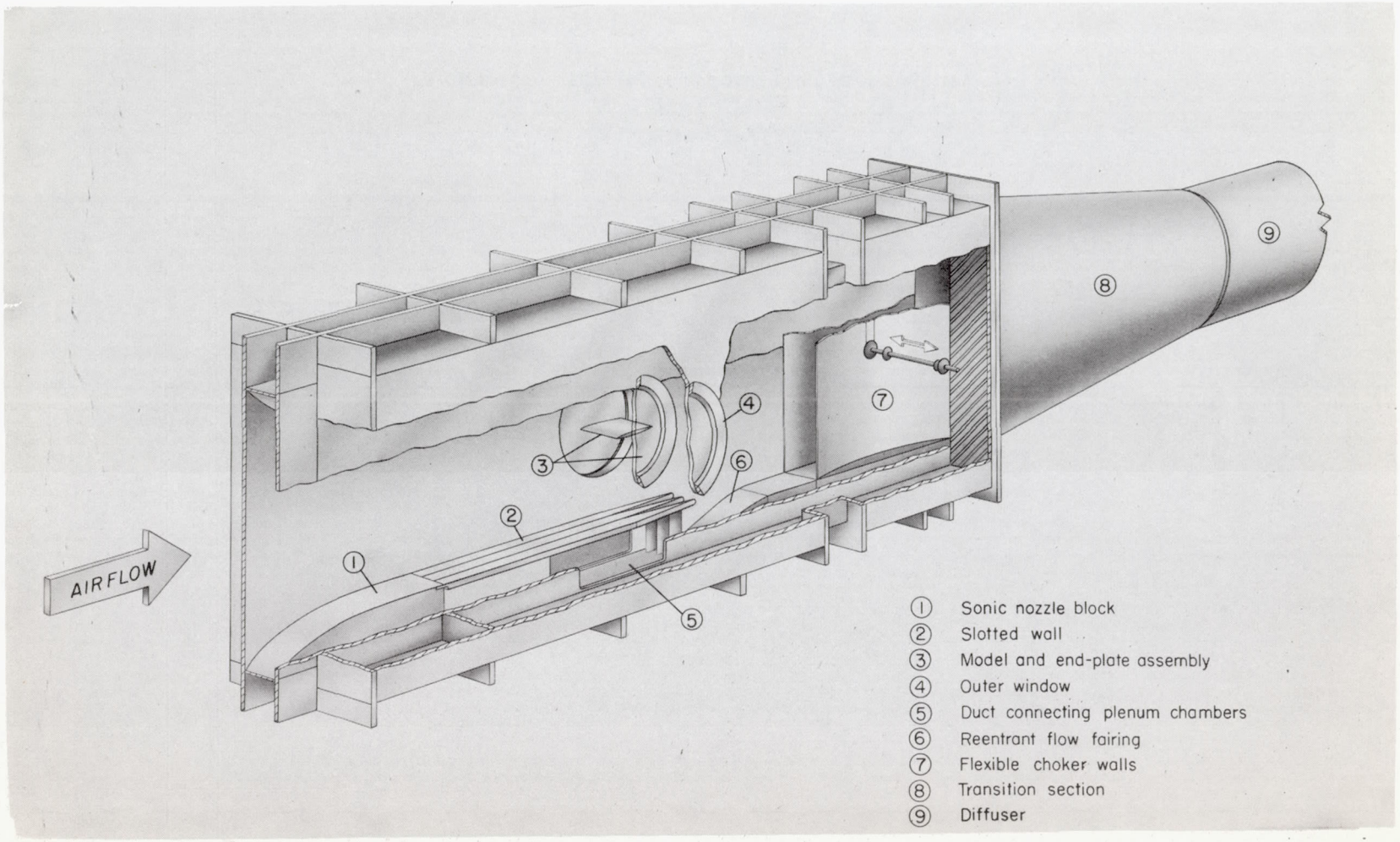
5. The Staff of The Ames 1- by 3-Foot Supersonic Wind-Tunnel Section: Notes and Tables for Use in the Analysis of Supersonic Flow. NACA TN 1428, 1947.

6. Humphreys, Milton D.: Pressure Pulsations on Rigid Airfoils at Transonic Speeds. NACA RM L51I12, 1951.



(a) General view.

Figure 1.- Langley airfoil test apparatus.



(b) Test section.

Figure 1.- Concluded.

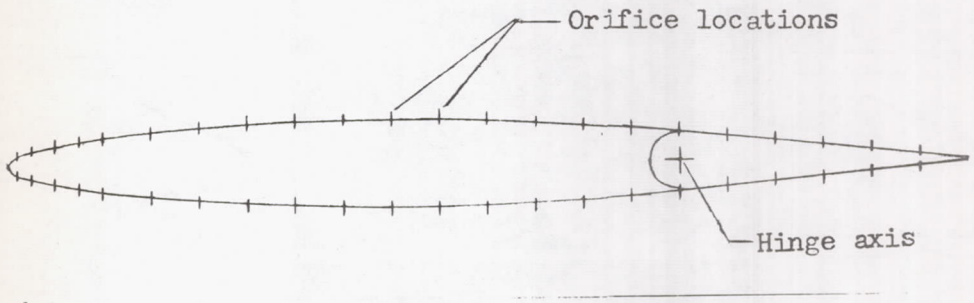


Figure 2.- NACA 65A009 profile with orifice locations.

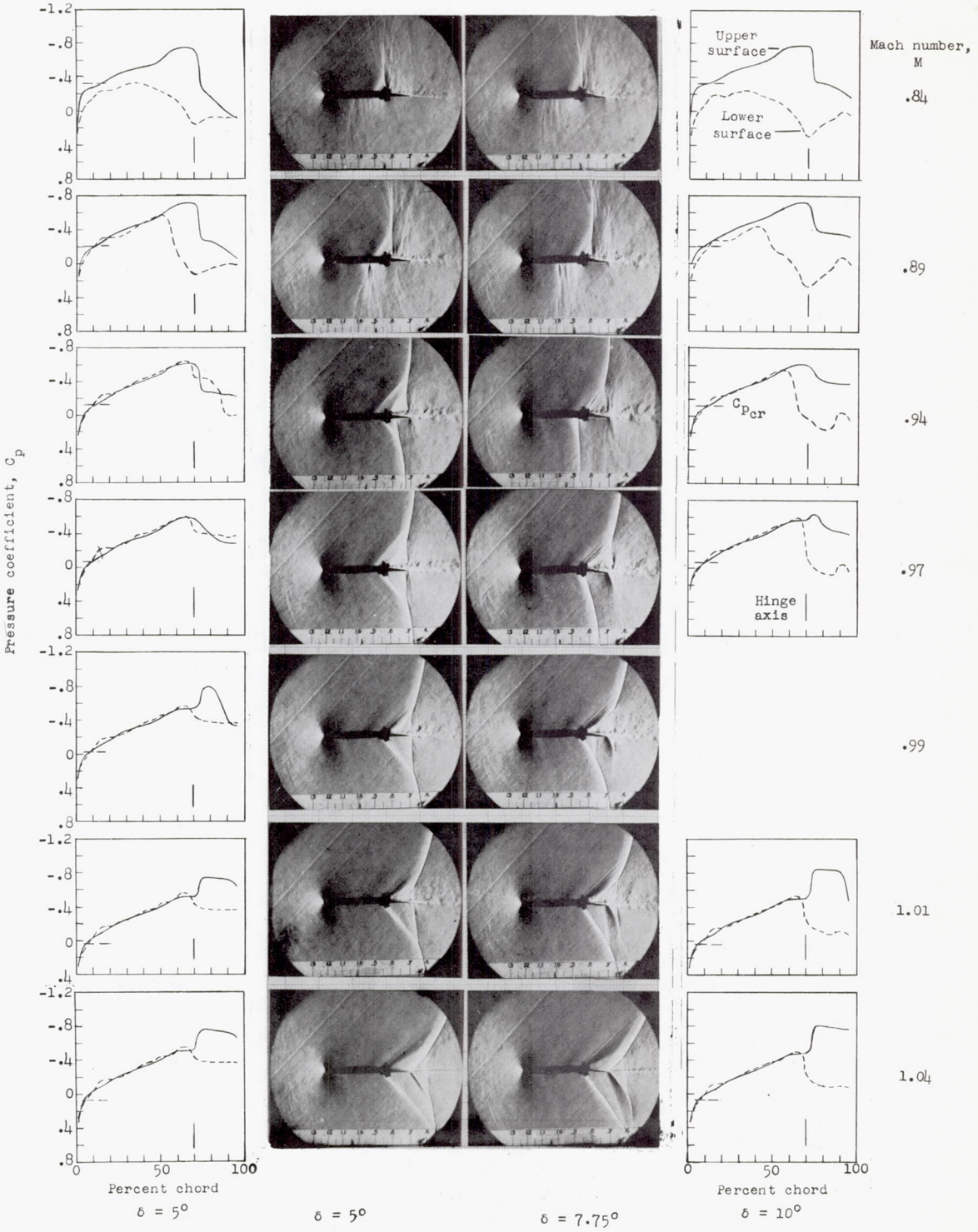
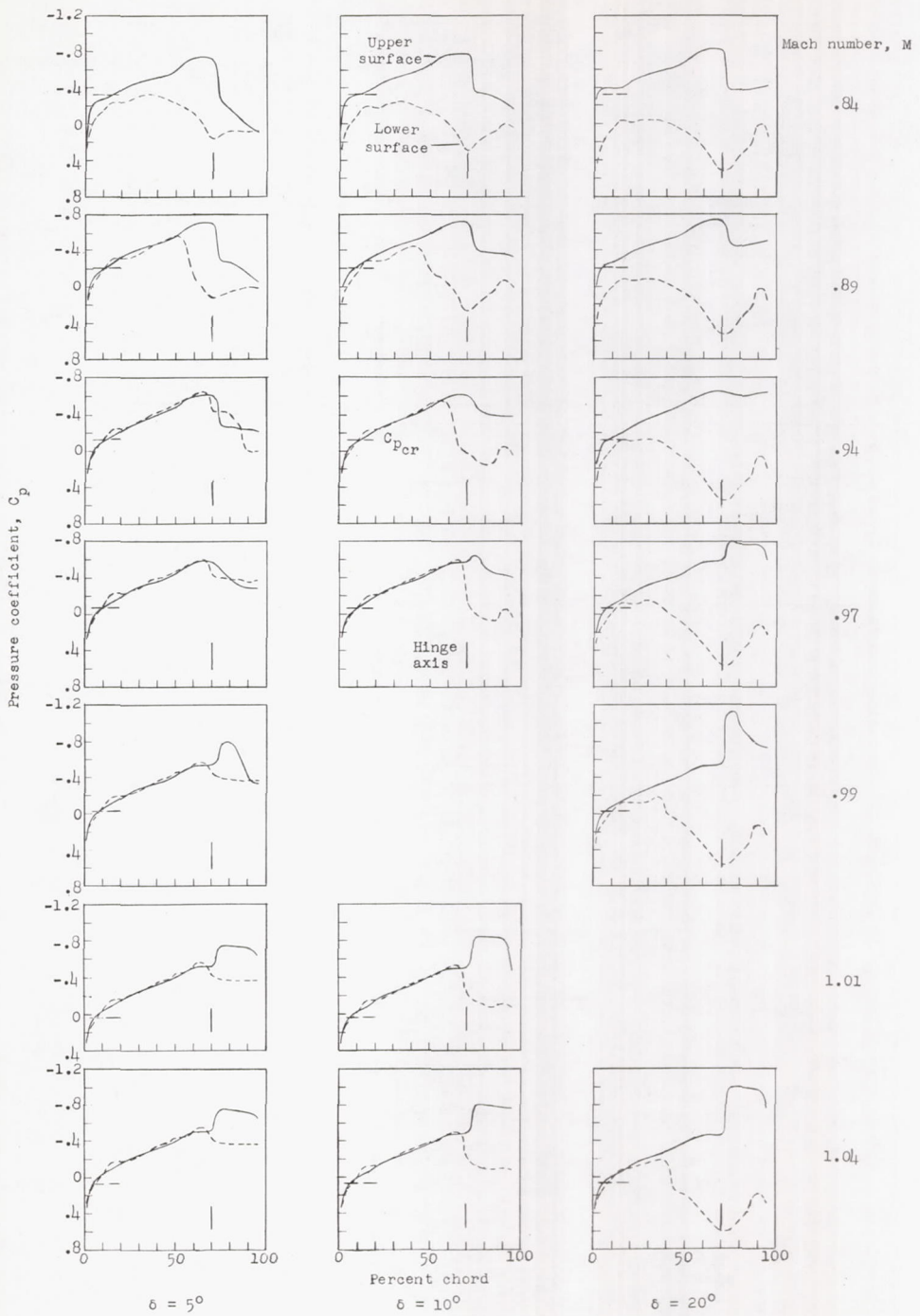
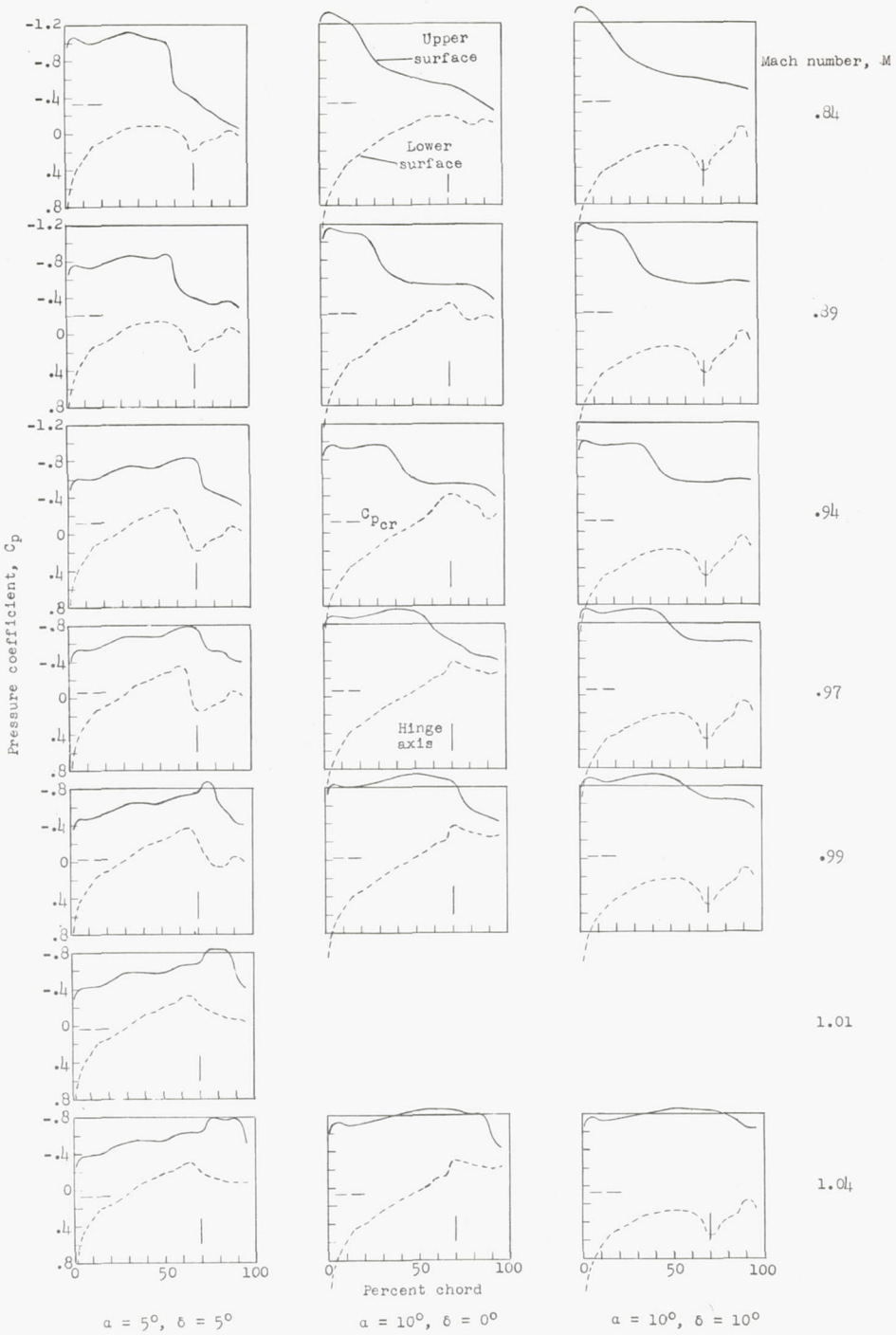


Figure 3.- Effects of flap deflection on flow. $\alpha = 0^\circ$. L-95897



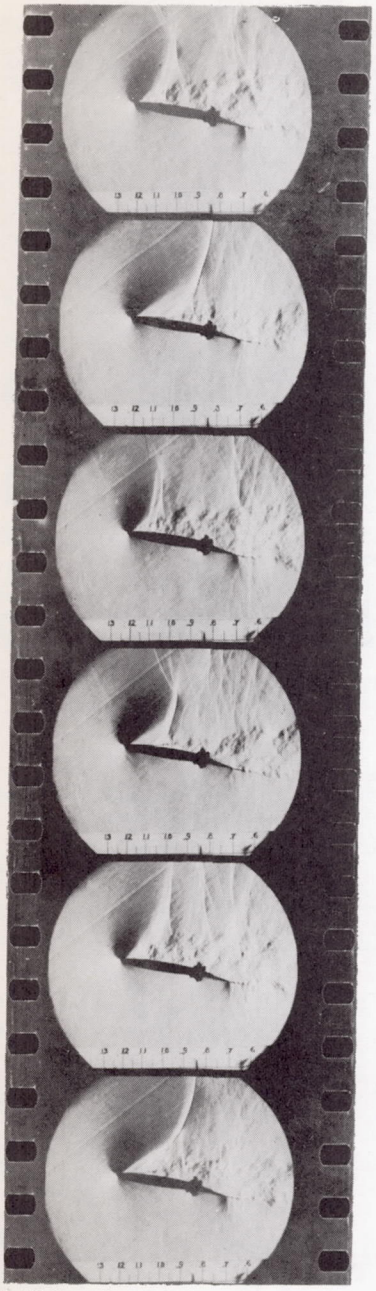
(a) $\alpha = 0^\circ$.

Figure 4.- Effects of flap deflection on pressure distributions.

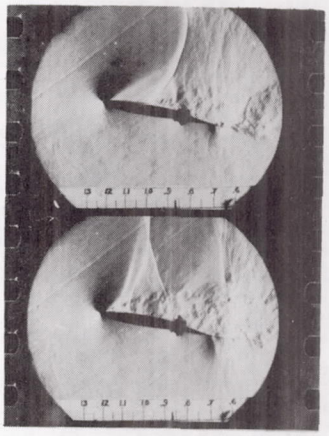


(b) $\alpha > 0^\circ$.

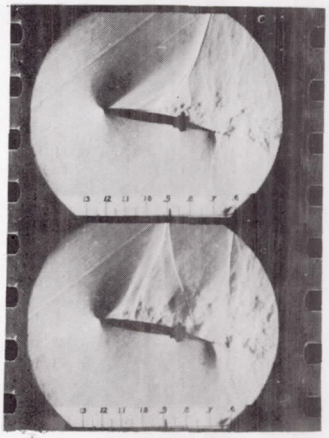
Figure 4.- Concluded.



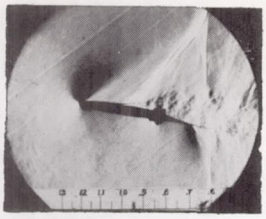
M = 0.84



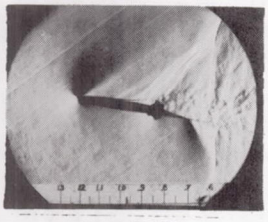
M = 0.87



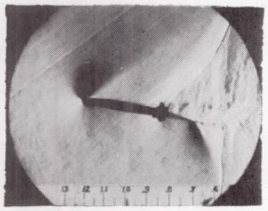
M = 0.89



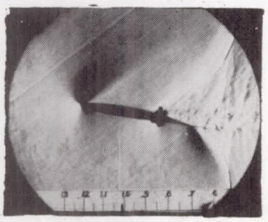
M = 0.94



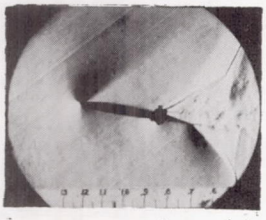
M = 0.97



M = 0.99



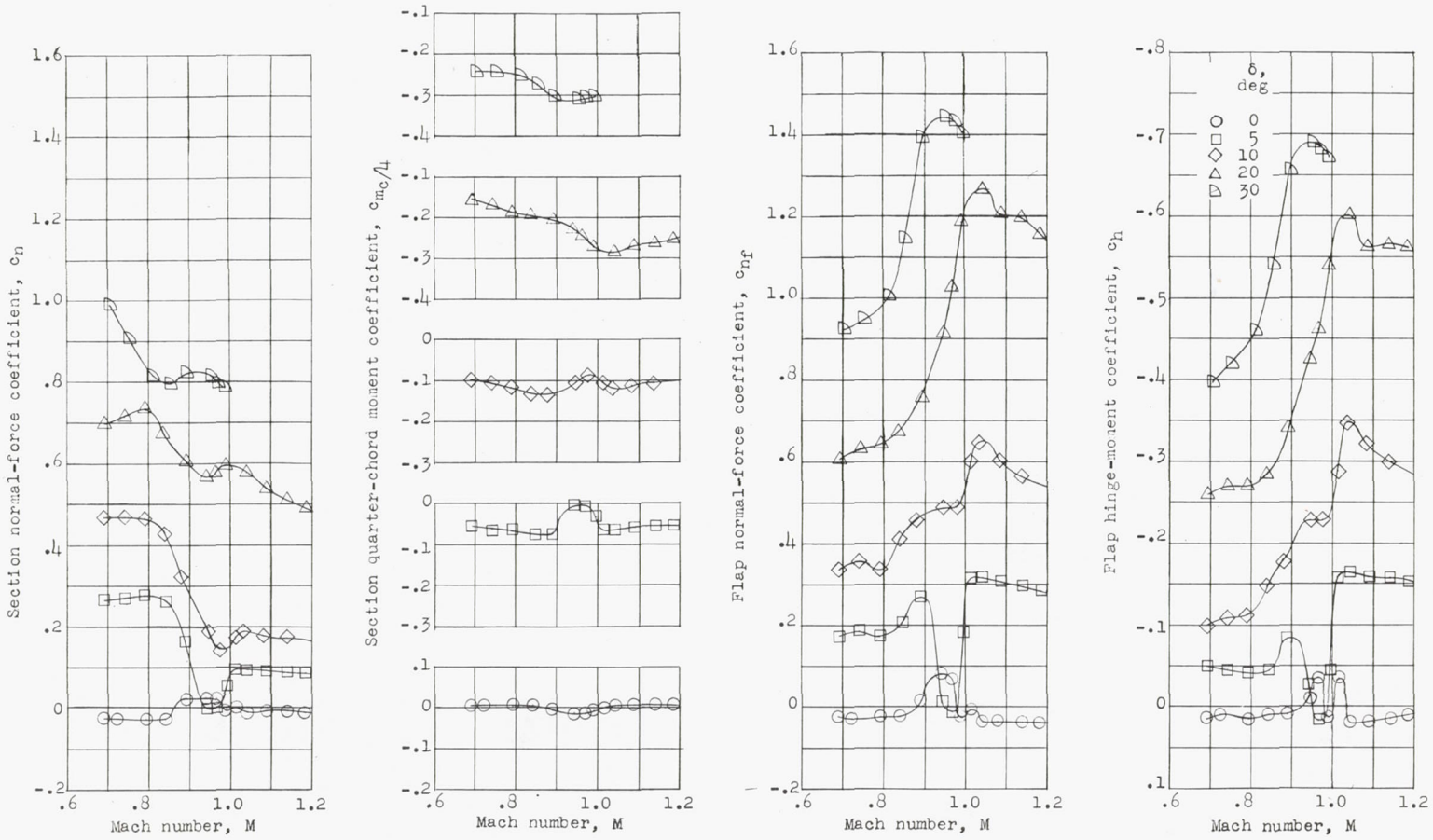
M = 1.01



M = 1.04

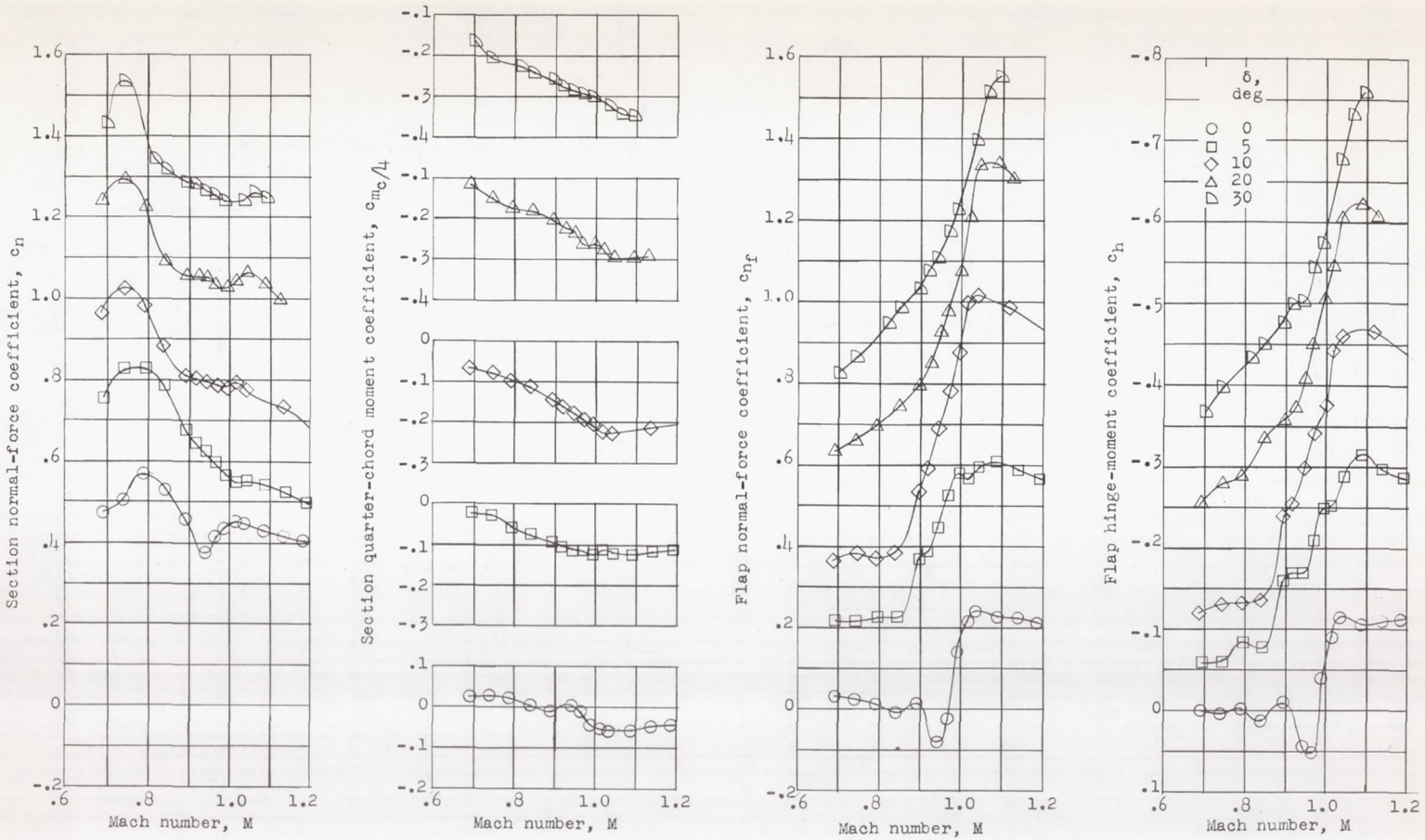
L-95898

Figure 5.- Schlieren photographs of flow past model. $\alpha = 10^{\circ}$; $\delta = 7.75^{\circ}$.



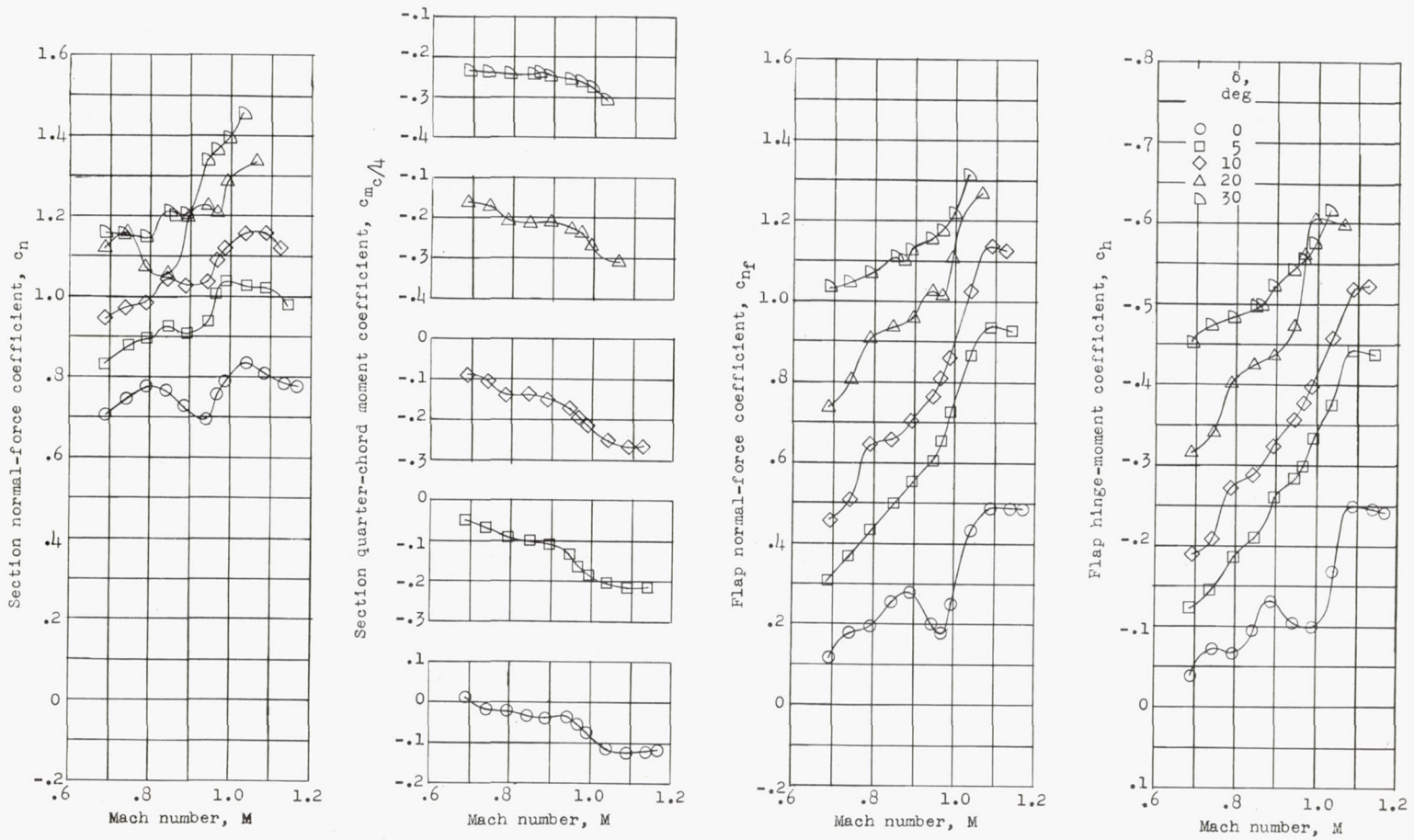
(a) $\alpha = 0^\circ$.

Figure 6.- Effects of flap deflection on airfoil characteristics.



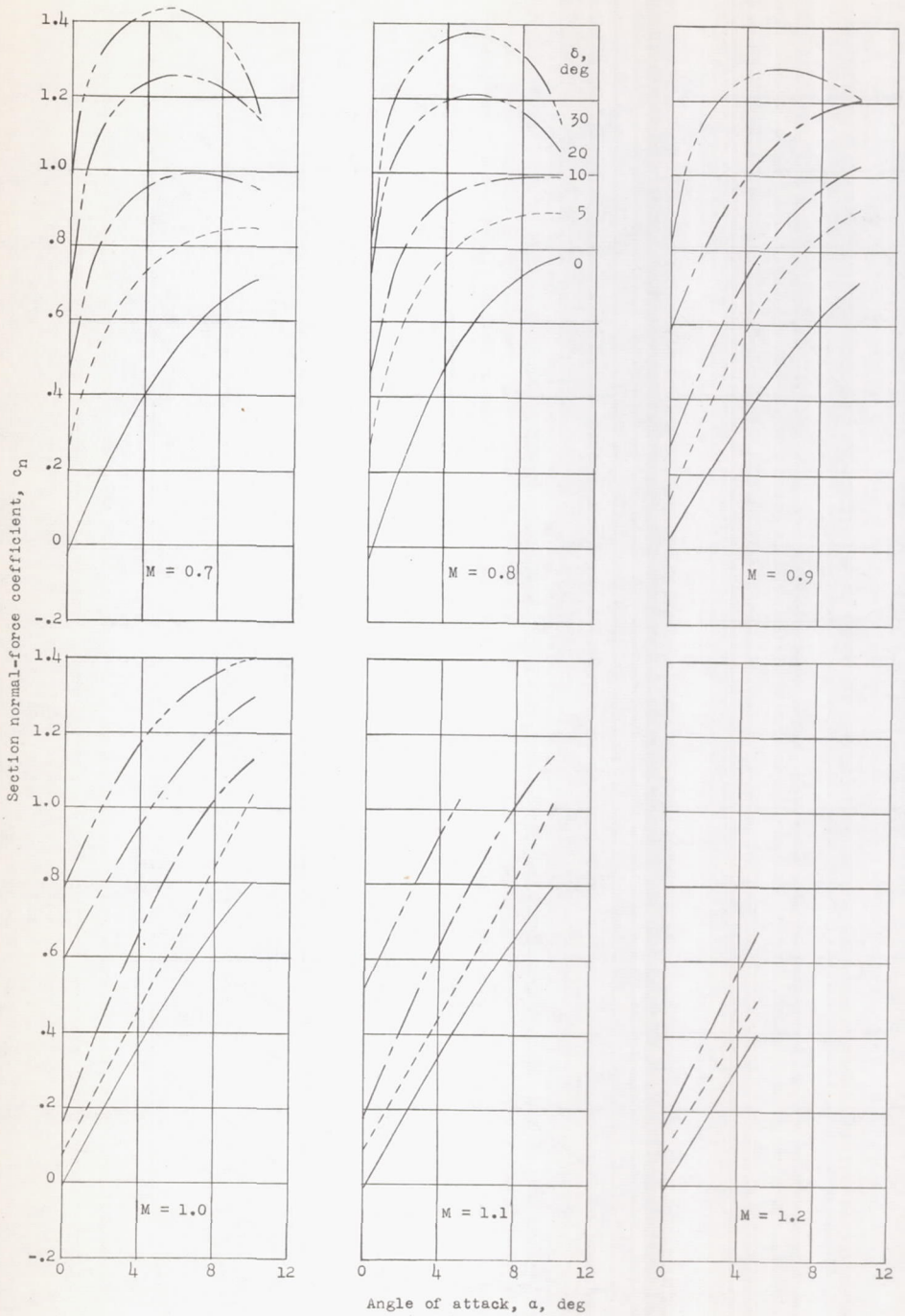
(b) $\alpha = 5°$.

Figure 6.- Continued.



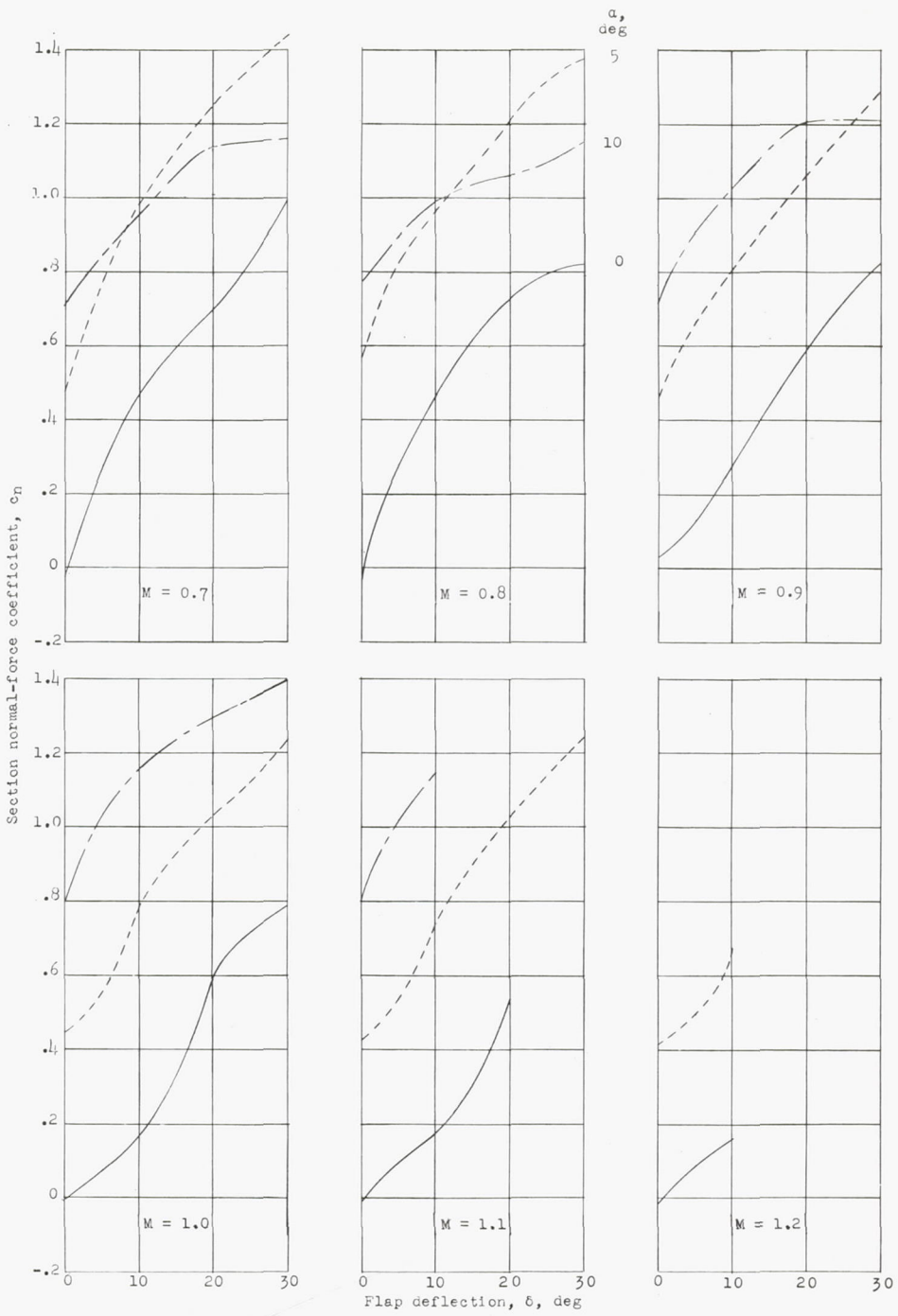
(c) $\alpha = 10^{\circ}$.

Figure 6.- Concluded.



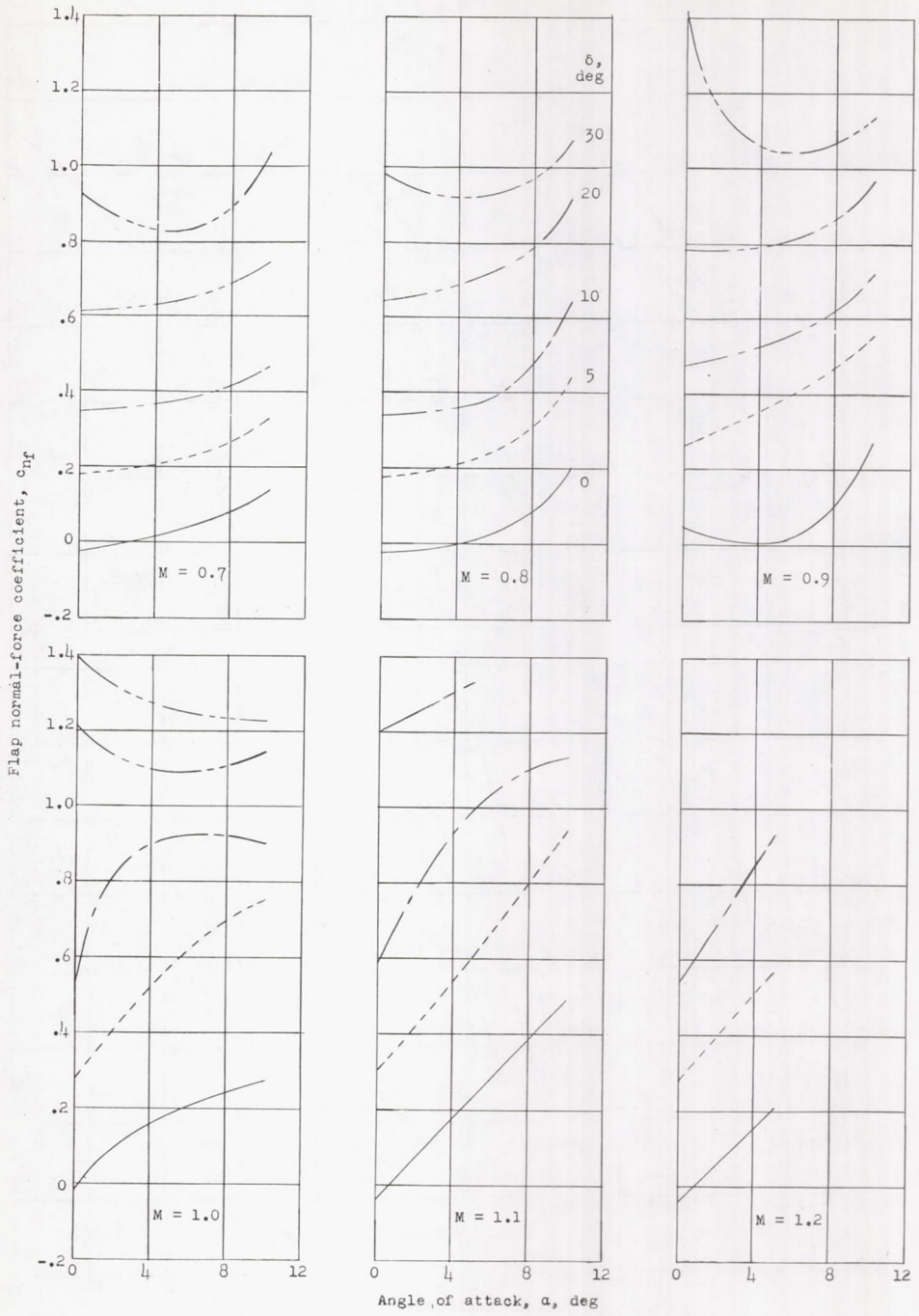
(a) Variation with angle of attack.

Figure 7.- Airfoil section normal-force characteristics.



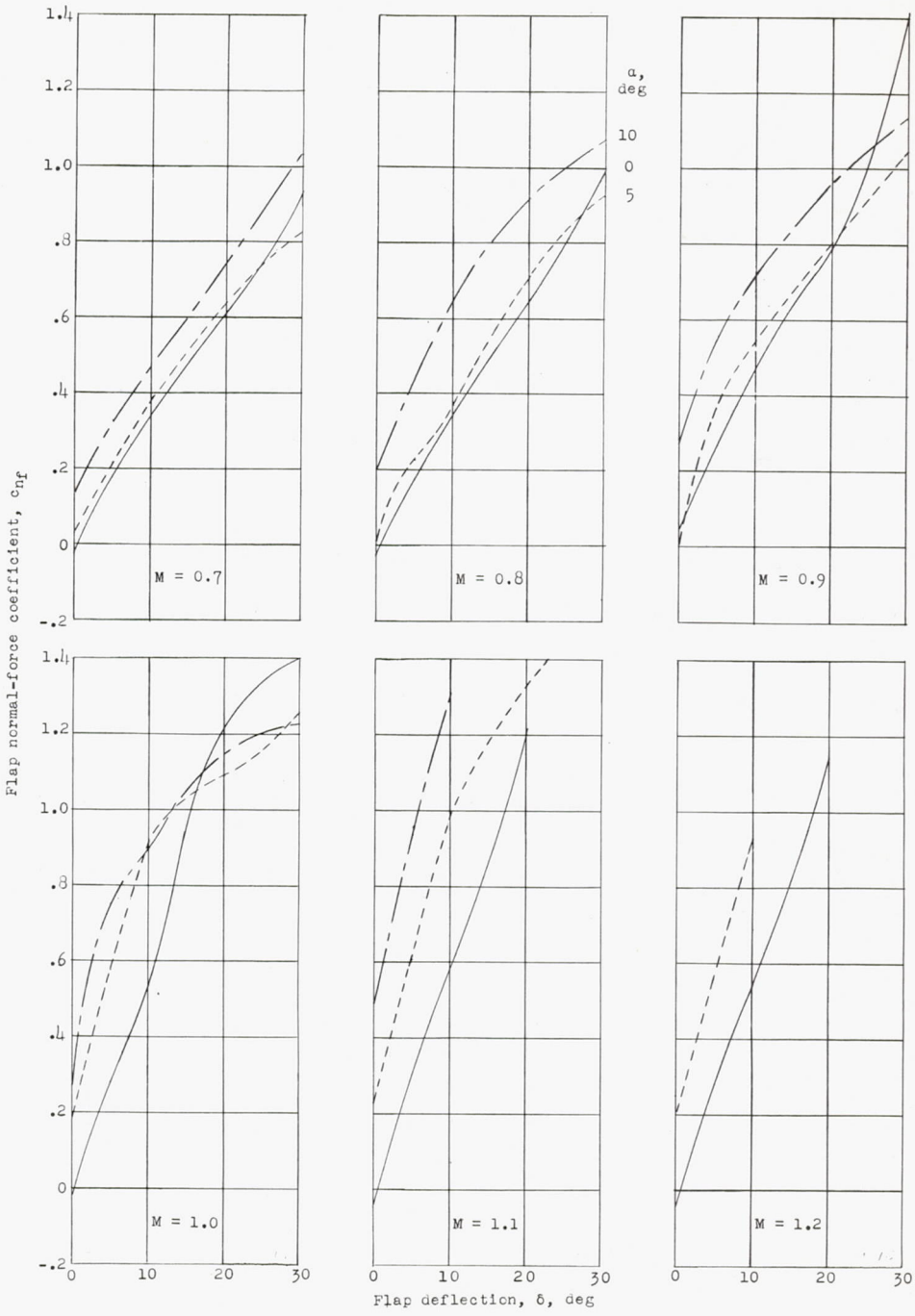
(b) Variation with flap deflection.

Figure 7.- Concluded.



(a) Variation with angle of attack.

Figure 8.- Flap normal-force characteristics.



(b) Variation with flap deflection.

Figure 8.- Concluded.

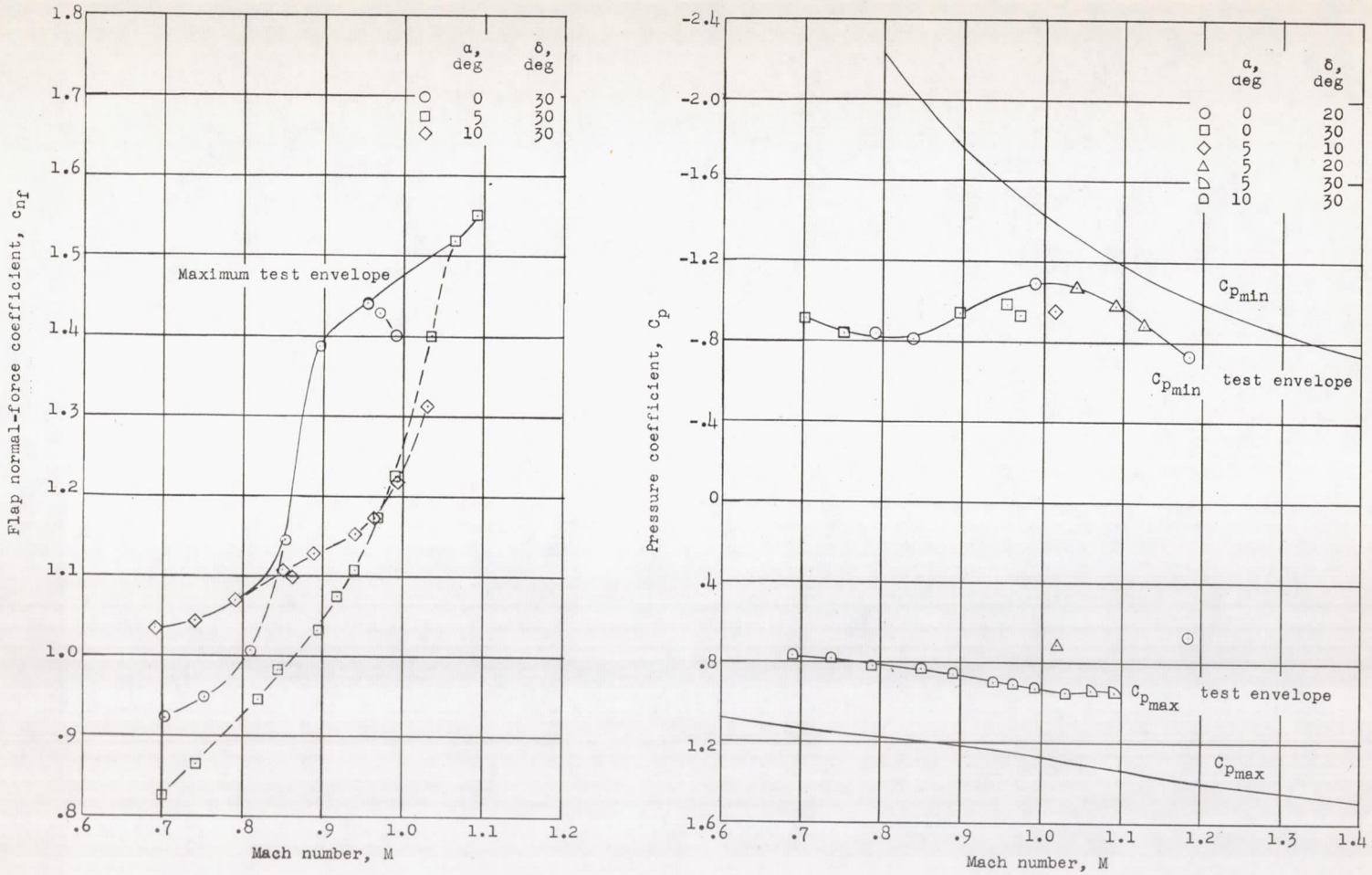


Figure 9.- Flap loads.

NACA - Langley Field, Va.